NEON ALGORITHM THEORETICAL BASIS DOCUMENT (ATBD) – NET RADIOMETER

PREPARED BY	ORGANIZATION	DATE
Derek Smith	FIU	07/02/2013
Josh Roberti	FIU	09/22/2015
Natchaya Pingintha-Durden	FIU	01/09/2015
Jesse Vance	AQU	02/08/2015
Cove Sturtevant	FIU	11/07/2016
Kaelin M. Cawley	AQU	05/24/2017
Rommel Zulueta	FIU	03/30/2020

APPROVALS	ORGANIZATION	APPROVAL DATE
Kate Thibault	SCI	05/16/2022

RELEASED BY	ORGANIZATION	RELEASE DATE
Tanisha Waters	CM	05/16/2022

See configuration management system for approval history.

The National Ecological Observatory Network is a project solely funded by the National Science Foundation and managed under cooperative agreement by Battelle. Any opinions, findings, and conclusions or recommendations expressed in this material are those of the author(s) and do not necessarily reflect the views of the National Science Foundation.

Change Record

REVISION	DATE	ECO #	DESCRIPTION OF CHANGE
A	08/28/2013	ECO-00922	Initial Release
B	10/23/2015	ECO-03110	Updated document to reflect L0 and L1 data product renumbering Revised *Algorithm Implementation* and *Uncertainty* Sections Added aquatic meteorology station information.
C	12/20/2017	ECO-05281	implemented standardized coverage factor of k=2 Moved consistency analyses outline to Future Plans / Modifications Sections Added information related to buoy specific data product DP1.20032
D	03/27/2020	ECO-06414	Removed mention of de-spiking algorithm for shortwave radiation streams. Added a note that the persistence test is only applied during local, daylight hours for shortwave radiation streams
E	05/16/2022	ECO-06813	• Added NEON to document title • Minor formatting updates

TABLE OF CONTENTS

LIST OF TABLES AND FIGURES

1 DESCRIPTION

Contained in this document are details concerning net radiation measurements made at all NEON sites. Incoming and outgoing long wave (LW) and short wave (SW) radiation will be measured via the net radiometer discussed here. Specifically, the algorithm process necessary to convert "raw" sensor measurements into meaningful scientific units and their associated uncertainties are described.

1.1 Purpose

This document details the algorithms used for creating NEON Level 1 data product from Level 0 data, and ancillary data as defined in this document (such as calibration data), obtained via instrumental measurements made by the net radiometer. It includes a detailed discussion of measurement theory and implementation, appropriate theoretical background, data product provenance, quality assurance and control methods used, approximations and/or assumptions made, and a detailed exposition of uncertainty resulting in a cumulative reported uncertainty for this product.

1.2 Scope

The theoretical background and entire algorithmic process used to derive Level 1 data from Level 0 data for the net radiometer are described in this document. It is expected that the net radiometer employed at all NEON tower sites is the Hukseflux NR01 (NEON part number: 0300070002). This document does not provide computational implementation details, except for cases where these stem directly from algorithmic choices explained here.

2 RELATED DOCUMENTS, ACRONYMS AND VARIABLE NOMENCLATURE

2.1 Applicable Documents

AD[01]	NEON.DOC.000001	NEON Observatory Design
AD[02]	NEON.DOC.005003	NEON Scientific Data Products Catalog
AD[03]	NEON.DOC.002652	NEON Level 1-3 Data Products Catalog
AD[04]	NEON.DOC.005005	NEON Level 0 Data Products Catalog
AD[05]	NEON.DOC.000782	NEON ATBD QA/QC data consistency
AD[06]	NEON.DOC.011081	ATBD QA/QC plausibility tests
AD[07]	NEON.DOC.000783	ATBD QA/QC Time Series Signal Despiking for TIS Level 1 Data Products
AD[08]	NEON.DOC.000802	NR01 – Net Radiometer Calibration/Validation Procedure
AD[09]	NEON.DOC.000849	C^3 Net Radiometer
AD[10]	NEON.DOC.000927	NEON Calibration and Sensor Uncertainty Values[1]
AD[11]	NEON.DOC.000785	TIS Level 1 Data Products Uncertainty Budget Estimation Plan
AD[12]	NEON.DOC.000751	CVAL Transfer of standard procedure
AD[13]	NEON.DOC.000746	Evaluating Uncertainty (CVAL)
AD[14]	NEON.DOC.002002	Engineering Master Location Sensor Matrix
AD[15]	NEON.DOC.001113	Quality Flags and Quality Metrics for TIS Data Products
AD[16]	NEON.DOC.001452	C^3 AQU Net Radiometer
AD[17]	NEON.DOC.001152	Aquatic Sampling Strategy
AD[18]	NEON.DOC.003808	C^3 Buoy meteorological station and submerged sensor assembly
AD[19]	NEON.DOC.004395	Net radiation on-buoy ingest workbook
AD[20]	NEON.DOC.004396	Net radiation on-buoy publication workbook
AD[21]	NEON.DOC.002651	NEON Data Product Numbering Convention

2.2 Reference Documents

RD[01]	NEON.DOC.000008	NEON Acronym List
RD[02]	NEON.DOC.000243	NEON Glossary of Terms

2.3 Acronyms

Acronym	Explanation
ATBD	Algorithm Theoretical Basis Document

[1] Note that CI obtains calibration and sensor values directly from an XML file maintained and updated by CVAL in real time. This report is updated approximately quarterly such that there may be a lag time between the XML and report updates.

CVAL	**NEON Calibration, Validation, and Audit Laboratory**
DAS	**Data Acquisition System**
DP	Data Product
L0	Level 0
L1	Level 1
PRT	Platinum Resistance Thermometer
UQ	Unquantifiable Uncertainty

2.4 Variable Nomenclature

The symbols used to display the various inputs in the ATBD, e.g., calibration coefficients and uncertainty estimates, were chosen so that the equations can be easily interpreted by the reader. However, the symbols provided will not always reflect NEON's internal notation, which is relevant for Cyberinfrastructure's (CI's) use, and or the notation that is used to present variables on NEON's data portal. Therefore a lookup table is provided in order to distinguish what symbols specific variables can be tied to in the following document.

Symbol	Internal Notation	Description
α_{u0}	CVALA0	CVAL upward facing pyrgeometer sensor sensitivity coefficient
α_{u1}	CVALA1	CVAL upward facing pyrgeometer sensor sensitivity coefficient
α_{u2}	CVALA2	CVAL upward facing pyrgeometer sensor sensitivity coefficient
α_{d0}	CVALA0	CVAL downward facing pyrgeometer sensor sensitivity coefficient
α_{d1}	CVALA1	CVAL downward facing pyrgeometer sensor sensitivity coefficient
α_{d2}	CVALA2	CVAL downward facing pyrgeometer sensor sensitivity coefficient
β_u	CVALA1	CVAL upward facing pyranometer sensor sensitivity coefficient
β_d	CVALA1	CVAL downward facing pyranometer sensor sensitivity coefficient
O_R	U_CVALR4	offset imposed by the FDAS for resistance readings (Ω)
O_V	U_CVALV4	offset imposed by the FDAS for voltage readings (V)
$u_{A1,Pu}$	U_CVALA1	Combined, relative calibration uncertainty of incoming shortwave radiation (%)
$u_{A1,Pd}$	U_CVALA1	Combined, relative calibration uncertainty of outgoing shortwave radiation (%)
$u_{A1,Uu}$	U_CVALA1	Combined, standard calibration uncertainty of incoming longwave radiation (W m^{-2})
$u_{A1,Ud}$	U_CVALA1	Combined, standard calibration uncertainty of outgoing longwave radiation (W m^{-2})
$u_{A3,Pu}$	U_CVALA3	Combined, relative calibration uncertainty (truth and trueness) of incoming shortwave radiation (%)

$u_{A3,Pd}$	U_CVALA3	Combined, relative calibration uncertainty (truth and trueness) of outgoing shortwave radiation (%)
$u_{A3,Uu}$	U_CVALA3	Combined, standard calibration uncertainty (truth and trueness) of incoming longwave radiation (W m^{-2})
$u_{A3,Ud}$	U_CVALA3	Combined, standard calibration uncertainty (truth and trueness) of outgoing longwave radiation (W m^{-2})
u_{R1}	U_CVALR1	Combined, relative uncertainty of Field DAS resistance readings (%)
u_{R3}	U_CVALR3	Combined, relative uncertainty (truth and trueness only) of Field DAS resistance readings (%)
u_{V1}	U_CVALV1	Combined, relative uncertainty of Field DAS voltage readings (%)
u_{V3}	U_CVALV3	Combined, relative uncertainty (truth and trueness only) of Field DAS voltage readings (%)

2.5 Verb Convention

"Shall" is used whenever a specification expresses a provision that is binding. The verbs "should" and "may" express non-mandatory provisions. "Will" is used to express a declaration of purpose on the part of the design activity.

3 DATA PRODUCT DESCRIPTION

3.1 Variables Reported

Net radiometer-related L1 DPs provided by the algorithms documented in this ATBD are displayed in the accompanying file nrd_datapub_NEONDOC002857.txt (NEON.DP1.00023).

Net radiometer-related L1 DPs for net radiation on-buoy (NEON.DP1.20032) can be found in the accompanying publication workbook AD[20], netRadBuoy_datapub_NEONDOC004396.txt.

3.2 Input Dependencies

Table 1 and **Table 2** details the net radiometer-related L0 DPs used to produce L1 DPs via this ATBD.

Table 1. List of net radiometer-related L0 DPs that are transformed into L1 DPs (DP1.00023) via this ATBD.

Description	Sample Frequency	Units	Data Product Number
Upward facing pyranometer (P_u)	1 Hz	V	NEON.DOM.SITE.DP0.00023.001.01315.HOR.VER.000
Downward facing pyranometer (P_d)	1 Hz	V	NEON.DOM.SITE.DP0.00023.001.01316.HOR.VER.000
Upward facing pyrgeometer (U_u)	1 Hz	V	NEON.DOM.SITE.DP0.00023.001.01317.HOR.VER.000
Downward facing pyrgeometer (U_d)	1 Hz	V	NEON.DOM.SITE.DP0.00023.001.01318.HOR.VER.000
Sensor body PRT resistance at temperature T (R_t)	1 Hz	Ω	NEON.DOM.SITE.DP0.00023.001.01314.HOR.VER.000
Heater Flag (QF_H)	1 Hz	NA	NEON.DOM.SITE.DP0.00023.001.01319.HOR.VER.000

Table 2. List of net radiometer-related L0 DPs that are transformed into L1 DPs (net radiation on-buoy DP1.20032) via this ATBD.

Description	Sample Frequency	Units	Data Product Number
Upward facing pyranometer (P_u)	~1 per 30 seconds	volt	NEON.DOM.SITE.DP0.20032.001.01315.HOR.VER.000
Downward facing pyranometer (P_d)	~1 per 30 seconds	volt	NEON.DOM.SITE.DP0.20032.001.01316.HOR.VER.000
Upward facing pyrgeometer (U_u)	~1 per 30 seconds	volt	NEON.DOM.SITE.DP0.20032.001.01317.HOR.VER.000

Downward facing pyrgeometer (U_d)	~1 per 30 seconds	volt	NEON.DOM.SITE.DP0.20032.001.01318.HOR.VER.000
Sensor body PRT resistance at temperature T (R_t)	~1 per 30 seconds	ohm	NEON.DOM.SITE.DP0.20032.001.01314.HOR.VER.000
Heater Flag (*QF_H*)	~1 per 30 seconds	NA	NEON.DOM.SITE.DP0.20032.001.01319.HOR.VER.000

3.3 Product Instances

A Hukseflux NR01 will be deployed on all core and re-locatable towers and aquatic met stations. Additionally, a Hukseflux NR01 will be deployed in the central most plot of the soil array at all tower sites, which will measure *only* incoming and outgoing LW radiation at the soil surface.

With slightly different configuration, a Hukseflux NR01 sensor will be deployed at all lake and river sites where the sensor will be installed on the buoy.

3.4 Temporal Resolution and Extent

One- and thirty-minute averages of SW and LW radiation will be calculated to form L1 DPs.

3.5 Spatial Resolution and Extent

Net radiometers will be deployed at the top level of the tower infrastructure and the central most plot of the soil array at all core and re-locatable tower sites. Net radiometers will be deployed at a standard height of 3 m above ground level at all aquatic sites. In addition, net radiometers will be deployed on the buoys at lake and river sites. Thus, NR01 measurements will represent the point in space where the measurement is taken. See AD[14] for site specific sensor location details.

4 SCIENTIFIC CONTEXT

The sun's energy is emitted to the earth mainly in the form of incoming short-wave (SW) radiation, with a small portion of it falling into incoming LW radiation wavelengths. Approximately 50% of the sun's emitted energy lies in the infrared wavelengths, between 0.7 and 5 µm. Of the remaining radiant energy from the sun, around 40% can be found in the visible region (i.e., 0.4-0.7 µm) and 10% in the ultraviolet region (i.e. <0.4 µm) (Fu, 2003; Goody and Yung, 1995).

A fraction of incoming solar radiation is returned to space through either reflection or backscattering, which is known as albedo. The earth's albedo is presently around 31% (Fu, 2003). Thus, the bulk of the sun's radiation is absorbed by the earth's surface. A portion of the radiation absorbed by the earth is then re-emitted back into the atmosphere in the form of LW radiation. This re-emitted LW radiation can be absorbed by gases in the atmosphere and re-radiated back to the earth's surface. This re-radiation of LW radiation results in atmospheric warming, known as the greenhouse effect. As such, incoming and outgoing SW and LW radiation are principal drivers of the hydrologic and energy budgets. Thus, time-series studies of net radiation are of great interest to the scientific and broader community to understand rates of change and their potential implications.

4.1 Theory of Measurement

The Hukseflux NR01 is a passive net radiation sensor, which serves to measure four separate components of surface radiation. The radiometer uses thermopiles to determine SW and LW fluxes from small output voltages that are proportional to the incoming and outgoing SW and LW fluxes. The net radiometer consists of four main components; a pyranometer, pyrgeometer, PRT, and a heater.

The pyranometer is used to measure SW radiation flux ($300 < \lambda < 2800$ nm), and is composed of one upward and one downward facing thermopile to measure incoming and outgoing SW radiation. The thermopile in the pyranometer is encased in a glass dome, which limits the spectral response from 300 to 2800 nm and shields the thermopile from atmospheric convection. The pyrgeometer determines LW radiation in the range of $4500 < \lambda < 50000$ nm. One pyrgeometer will face upward and determine incoming LW radiation, while the other pyrgeometer will face the earth's surface and measure outgoing LW radiation. The pyrgeometer's thermopile is enclosed by a silicon window to inhibit radiation below 4500 nm from entering and to shield the thermopile from atmospheric convection.

The pyrgeometer sensor itself emits LW radiation. Thus, the pyrgeometer's thermopile measurements are composed of the incoming minus the sensor outgoing LW radiation. If we consider the sensor to be a black body, we apply the Stefan–Boltzmann law to determine the portion of LW radiation emitted by the sensor. To summarize, the Stefan–Boltzmann law states that radiation emitted by a black body object is directly proportional to the fourth power of the black body's temperature. A PRT housed in the sensor body will determine sensor body temperature. Thus, the PRT will allow the fraction of LW radiation emitted by the pyrgeometer to be measured. The last component of the net radiometer is a heater, which is used to prevent condensation from developing on the sensor.

4.2 Theory of Algorithm

In addition to the thermopile outputs from the upward and downward facing pyranometers and pyrgeometers, sensor specific sensitivities are needed to derive values for SW and LW radiation. The sensor specific sensitivities are determined by CVAL according to AD[08]. As previously mentioned, sensor body temperature is needed to determine incoming and outgoing LW radiation. This is due to the LW radiation that is emitted by the pyrgeometer, and thus the thermopile measurements represent incoming minus the portion of LW radiation that is emitted. Sensor body temperature will be determined from the PRT using two separate equations; one equation for temperatures < 0 °C, Eq. (2), and one for temperatures ≥ 0 °C, Eq. (3), (ASTM, 2004). The raw resistance received from the PRT will identify which equation will be used to determine the temperature (*T*) accordingly:

$$T = \begin{cases} \text{Eq.}(2) & \text{if} \quad (\mathrm{R_t} < 100\ \Omega) \\ \text{Eq.}(3) & \text{if} \quad (\mathrm{R_t} \geq 100\ \Omega) \end{cases} \tag{1}$$

The non-linearity of a PRT can be expressed as follows for resistance < 100 [Ω] as (ASTM, 2004):

$$T_i = \sum_{k=1}^{4} D_k \left(R_{t_i}/R_0 - 1\right)^k \tag{2}$$

Where,

T_i = Individual (1 Hz) Temperature (°C)
R_{t_i} = Individual PRT resistance at temperature, *T* (Ω)
R_0 = 100 (Ω) [Nominal resistance at 0 °C defined as 100 Ω for a PRT 100]
D_1 = 255.819 (°C) [coefficient defined by ASTM – E 1137/E 1137M]
D_2 = 9.14550 (°C) [coefficient defined by ASTM – E 1137/E 1137M]
D_3 = -2.92363 (°C) [coefficient defined by ASTM – E 1137/E 1137M]
D_4 = 1.79090 (°C) [coefficient defined by ASTM – E 1137/E 1137M]

Likewise, for resistance ≥ 100 [Ω] ASTM (2004) expresses PRTs' non-linearity as:

$$T_i = \frac{\left(A^2 - 4B\left(1 - R_{t_i}/R_0\right)\right)^{\frac{1}{2}} - A}{2B} \tag{3}$$

Where,

T_i = Individual (1 Hz) Temperature (°C)
R_{t_i} = Individual PRT resistance at temperature, *T* (Ω)
R_0 = 100 (Ω) [Nominal resistance at 0°C defined as 100 Ω for a PRT 100]
A = $3.9083 * 10^{-3}$ ($°C^{-1}$) [coefficient defined by IEC 751 and the ITS-90 scale]

B = -5.775*10^{-7} (°C^{-2}) [coefficient defined by IEC 751 and the ITS-90 scale]

Note: In the event that the International Temperature Scale (ITS) is updated from the ITS-90 scale, the coefficients listed above will be revised to reflect the most current ITS.

It is then necessary to convert temperature from Celsius to Kelvin as follows:

$$T(K) = T(°C) + 273.15\ \text{K} \tag{4}$$

Once sensor body temperature is resolved, individual, incoming and outgoing LW radiation is determined accordingly (NREL 2013):

$$L_{I_i} = \alpha_{u0} + \alpha_{u1} U_{u_i} + \alpha_{u2} \sigma_{SB} \left(T_i + c U_{u_i}\right)^4 \tag{5}$$

And

$$L_{O_i} = \alpha_{d0} + \alpha_{d1} U_{d_i} + \alpha_{d2} \sigma_{SB} \left(T_i + c U_{d_i}\right)^4 \tag{6}$$

Where,

L_{I_i} = Individual (1 Hz) Incoming Long Wave Radiation [W m^{-2}]
L_{O_i} = Individual Outgoing Long Wave Radiation [W m^{-2}]
U_{u_i} = Individual upward- facing pyrgeometer [V]
U_{d_i} = Individual downward- facing pyrgeometer [V]
α_{u0} = Upward facing pyrgeometer sensor sensitivity [W m^{-2}] provided by CVAL
α_{u1} = Upward facing pyrgeometer sensor sensitivity [W m^{-2} V^{-1}] provided by CVAL
α_{u2} = Upward facing pyrgeometer sensor sensitivity [unitless] provided by CVAL
α_{d0} = Downward facing pyrgeometer sensor sensitivity [W m^{-2}] provided by CVAL
α_{d1} = Downward facing pyrgeometer sensor sensitivity [W m^{-2} V^{-1}] provided by CVAL
α_{d2} = Downward facing pyrgeometer sensor sensitivity [unitless] provided by CVAL
σ_{SB} = 5.67*10^{-8} [Stefan-Boltzmann constant, W m^{-2} K^{-4}]
T_i = Sensor body temperature [K]
c = 704.4 [K V^{-1}]

Incoming and outgoing SW radiation is determined from the pyranometer as follows:

$$S_{I_i} = P_{u_i} \beta_u \tag{7}$$

And,

$$S_{O\,i} = P_{d_i}\beta_d \quad (8)$$

Where,

$S_{I\,i}$ = Incoming Short Wave Radiation (W m^{-2})
$S_{O\,i}$ = Outgoing Short Wave Radiation (W m^{-2})
P_{u_i} = Upward facing pyranometer (V)
P_{d_i} = Downward facing pyranometer (V)
β_u = Upward facing pyranometer sensor sensitivity (W m^{-2} V^{-1}) provided by CVAL
β_d = Downward facing pyranometer sensor sensitivity (W m^{-2} V^{-1}) provided by CVAL

One-minute and thirty-minute averages will be determined accordingly to create L1 DPs listed in file nrd_datapub_NEONDOC002857.txt. Here we let Rad represent incoming and outgoing LW and SW radiation since they will be averaged the same way:

$$\overline{Rad}_1 = \frac{1}{n}\sum_{i=1}^{n} Rad_i \quad (9)$$

where, for each 1-minute average, n is the number of measurements during the averaging period and Rad_i is a 1-Hz radiation measurement taken during the 60-second averaging period [0, 60). For a 1-minute average, n = 60 if all data points are included.

and

$$\overline{Rad}_{30} = \frac{1}{n}\sum_{i=1}^{n} Rad_i \quad (10)$$

where, for each 30-minute average, n is the number of measurements during the averaging period and Rad_i is a 1-Hz temperature measurement taken during the 1800-second averaging period [0, 1800).

Note: The beginning of the first averaging period in a series shall be the nearest whole minute less than or equal to the first timestamp in the series.

The buoy mounted Hukseflux NR01 returns data at about 1 measurement per 30 seconds. Because of the communication system at the buoys (AD[17]), it is possible that zero or more than one (probably 2 or 3 maximum) measurements will be returned per 30 seconds. Thus, for the buoy Hukseflux NR01 the number of values that are averaged may not be a consistent value. When zero measurements are returned for a given minute, a timestamp and data may not be published to users.

5 ALGORITHM IMPLEMENTATION

Data flow for signal processing of L1 DPs will be treated in the following order.

1. The net radiometer L0 DPs will be converted into incoming and outgoing SW and LW radiation through Eq. (1)-(8).
2. QA/QC Plausibility tests will be applied to the data stream in accordance with AD[06], details are provided below.
3. Signal de-spiking will be applied to the data stream (longwave radiation only) in accordance with AD[07].
4. One- and thirty-minute SW and LW radiation averages will be calculated using Eq. (9) and (10) and descriptive statistics, i.e. minimum, maximum, and variance, will be determined for averaging periods.
5. Quality metrics, quality flags, and the final quality flag will be produced for one- and thirty-minute averages according to AD[15].

QA/QC Procedure:

1. **Plausibility Tests** AD[08] – All plausibility tests will be determined for the net radiometer. Test parameters will be provided by FIU and maintained in the CI data store. All plausibility tests will be applied to the sensor's converted L0 DPs and an associated quality flags (QFs) will be generated for each test.

$$\overline{Rad}_{30} = \frac{1}{n}\sum_{i=x}^{n} Rad_i \qquad (11)$$

2. **Sensor Test** – A heater flag as identified in the C[3] document (AD[09]) will be applied to L0 DPs while the heater is operational. It is assumed that any heater-induced temperature changes in the sensor will be in equilibrium with the PRT. Therefore, any measurement variability induced by the heater, while it is on, will be accounted for by the internal PRT. One- and thirty-minute averages of quality metrics of the heater flag will be produced according to AD[15]. This offers a user greater transparency, as one will be able to identify the number of L0 DPs where the heater was on that went into creating the L1 DP.

3. **Signal De-spiking**– Time segments and threshold values for the automated de-spiking QA/QC routine will be specified by FIU and maintained in the CI data store. Flags from the de-spiking analysis will be applied according to AD[07]. Applicable for longwave radiation streams, only.

4. **Quality Flags (QFs) and Quality Metrics (QMs)** AD[15] – If a shortwave radiation datum has failed one of the following tests it will not be used to create a L1 DP: ***range, persistence, and step.*** It should be noted that the persistence test for shortwave radiation data streams is only applied during local, daylight hours. If a longwave radiation datum has failed one of the following tests it will not be used to create a L1 DP: range, persistence, step, and de-spiking. α and β QFs and QMs will be determined using the flags listed in **Table 3** except for the heater flag. In addition, L1 DPs will have a QA/QC report and quality metrics associated with each flag listed in **Table 3** as well as a final quality flag (***finalQF***), as detailed in AD[15]. Ancillary information needed for the algorithm and other information maintained in the CI data store is shown in **Table 4**.

Table 3. Flags associated with radiation measurements.

Flags
Range
Persistence
Step
Null
Gap
Valid Calibration
Signal De-spiking
Alpha
Beta
Final Quality Flag
Heater Flag

Table 4. Information maintained in the CI data store for the net radiometer.

Tests/Values	CI Data Store Contents
Range	Minimum and maximum values
Persistence	Window size, threshold values and maximum time length
Step	Threshold values
Null	Test limit
Gap	Test limit
Valid Calibration	CVAL sensor specific valid calibration date range
Signal Despiking	Time segments and threshold values
Calibration	CVAL sensor specific calibration coefficients AD[08]
Uncertainty	AD[10]
Sensor Test	AD[09]
Final Quality Flag	AD[15]

6 UNCERTAINTY

Uncertainty of measurement is inevitable; therefore, measurements should be accompanied by a statement of their uncertainty for completeness (JCGM 2008; Taylor 1997). To do so, it is imperative to identify all sources of measurement uncertainty related to the quantity being measured. Quantifying the uncertainty of TIS measurements will provide a measure of the reliability and applicability of individual measurements and TIS data products. This portion of the document serves to identify, evaluate, and quantify sources of uncertainty relating to individual, calibrated radiation measurements as well as L1 mean radiation data products. It is a reflection of the information described in AD[12], and is explicitly described for the radiation assembly in the following sections.

6.1 Uncertainty of Radiation Measurements

Uncertainty of the net radiometer assembly is discussed in this section. Discussion is broken down into two topics informing the discrepancy between the two types of uncertainty presented within this document. The first subsection details the sources of *measurement* uncertainty, i.e., those associated with *individual measurements*. The second discusses uncertainties associated with temporally averaged data products. A diagram detailing the data flow and known sources of uncertainty are displayed in **Figure 1**.

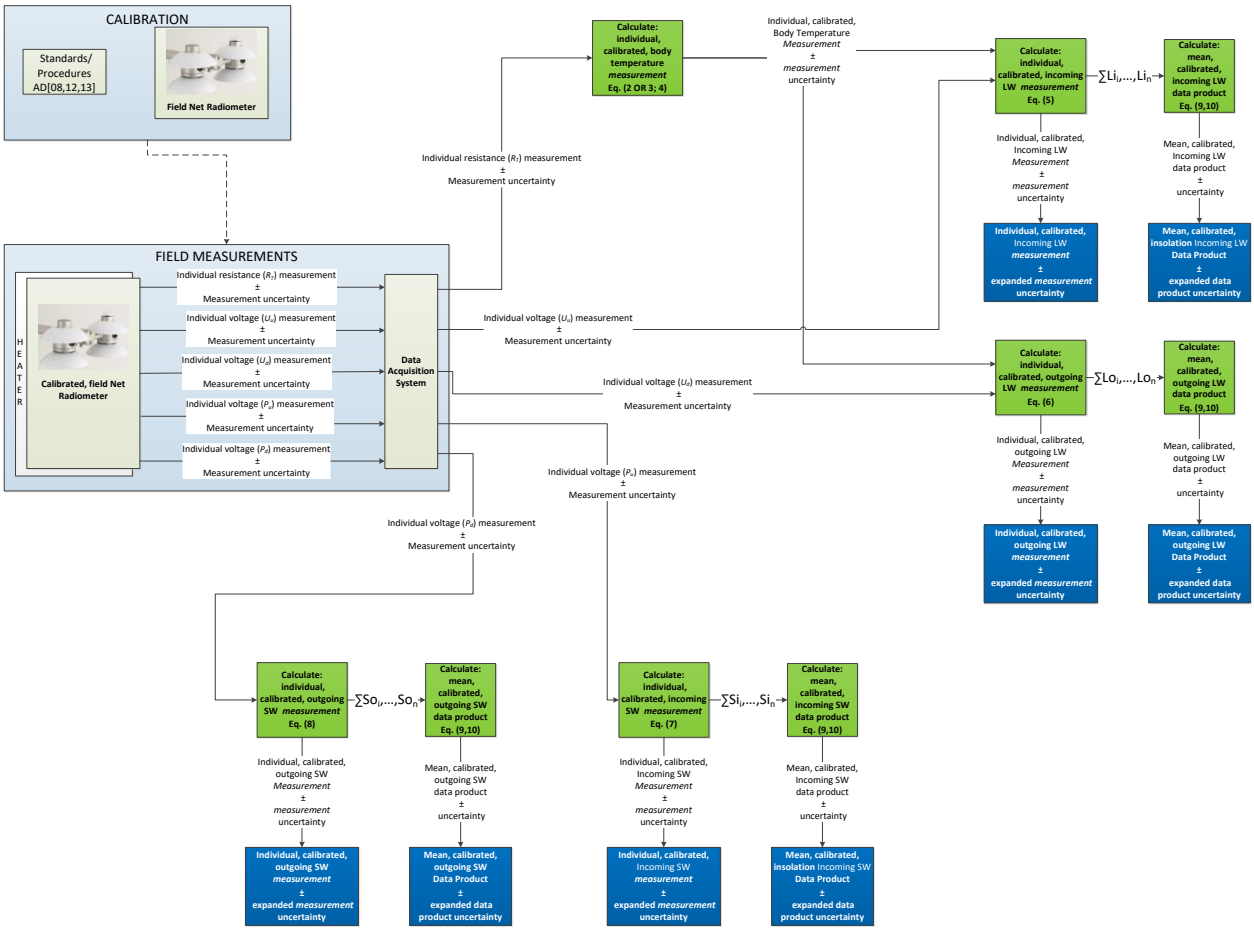

Figure 1. Displays the data flow and associated uncertainties of individual radiation measurements and L1 radiation DPs. For more information regarding the methods by which the net radiometer is calibrated, please refer to AD[08,12,13].

6.1.1 Measurement Uncertainty

The following subsections present the uncertainties associated with *individual observations*. It is important to note that the uncertainties presented in the following subsections are *measurement uncertainties*, that is, they reflect the uncertainty of an *individual* measurement. These uncertainties should not be confused with those presented in Section 6.1.2. We urge the reader to refer to AD[12] for further details concerning the discrepancies between quantification of measurement uncertainties and L1 uncertainties.

NEON calculates measurement uncertainties according to recommendations of the Joint Committee for Guides in Metrology (JCGM) 2008. In essence, if a measurand *y* is a function of *n* input quantities

x_i $(i = 1, \ldots, n)$, $i.e., y = f(x_1, x_2, \ldots, x_n)$, the combined measurement uncertainty of *y*, assuming the inputs are independent, can be calculated as follows:

$$u_c(y) = \left(\sum_{i=1}^{N} \left(\frac{\partial f}{\partial x_i} \right)^2 u^2(x_i) \right)^{\frac{1}{2}} \quad (12)$$

Where,

$\frac{\partial f}{\partial x_i}$ = partial derivative of *y* with respect to x_i

$u(x_i)$ = combined standard uncertainty of x_i.

Thus, the uncertainty of the measurand can be found be summing the input uncertainties in quadrature. The calculation of these input uncertainties is discussed below.

6.1.1.1 Calibration

CVAL (AD[10]) provides a combined, relative, measurement uncertainty for *each* shortwave radiation measurement stream, and a combined, standard measurement uncertainty for *each* longwave radiation stream. These uncertainties, i.e., $u_{A1,Pw}$, $u_{A1,Pd}$, (shortwave) $u_{A1,Uu}$, and $u_{A1,Ud}$ (longwave) represent i) the repeatability and reproducibility of the data stream and the lab DAS, and ii) uncertainty of the calibration procedures and coefficients including uncertainty in the standard (truth). Each will be stored in the CI data store. After converting the shortwave radiation uncertainties from (%) to measurement units (W m^{-2}), each will be applied to the respective, individual radiation measurements (that is, they do not vary with any specific sensor, DAS component, etc.). A detailed summary of the calibration procedures and corresponding uncertainty estimates can be found in AD [08,12,13].

The combined, standard, measurement uncertainty due to the calibration process is calculated as follows for the shortwave radiation measurement streams:

$$u_{CVAL}\left(S_{y_i}\right) = u_{A1,Pg} * S_{y\ i} \quad (13)$$

Where,

$u_{CVAL}\left(S_{y_i}\right)$ = partial uncertainty of shortwave radiation measurement resulting from sensor calibration (W m^{-2})

S_y = Incoming / outgoing (subscript 'y') shortwave (W m^{-2})

P_g = Incoming / outgoing (subscript 'g') shortwave radiation voltage output (V)

$u_{A1,Pg}$ = relative uncertainty of respective (incoming / outgoing) shortwave radiation stream; provided by CVAL (AD[10])

Note: Uncertainty values of longwave radiation do not need to be converted, as they are provided in W m^{-2}.

Internal body temperature *will not* be calibrated at NEON's CVAL, thus, CVAL will not supply an uncertainty value for this measurement. Please refer to Section 6.1.3 for further justification.

6.1.1.2 DAS

Uncertainty calculations for the Campbell CR1000 will use the same equations as those for the Grape data loggers. The uncertainty introduced by the Field DAS is computed via:

$$u_{FDAS}\left(\mathrm{W}_{g_i}\right) = \left(u_{V1} * \mathrm{W}_{g_i}\right) + O_V \tag{14}$$

And,

$$u_{FDAS}\left(\mathrm{R}_{T_i}\right) = \left(u_{R1} * \mathrm{R}_{T_i}\right) + O_R \tag{15}$$

Where,

$u_{FDAS}\left(\mathrm{W}_{g_i}\right)$ = combined, standard uncertainty of the respective voltage stream (W, either shortwave or longwave) introduced by the Field DAS (V)

$u_{FDAS}\left(\mathrm{R}_{T_i}\right)$ = combined, standard uncertainty of the resistance output introduced by the Field DAS (Ω)

W_g = respective voltage output (V)

R_T = resistance output (Ω)

$u_{V1,}$ = combined, relative Field DAS uncertainty for voltage measurements provided by CVAL (unitless)

u_{R1} = combined, relative Field DAS uncertainty for resistance measurements provided by CVAL (unitless)

O_V = offset (voltage) imposed by the FDAS provided by CVAL (V)

O_R = offset (resistance) imposed by the FDAS provided by CVAL (Ω)

To calculate the partial uncertainty of individual *longwave* radiation measurements resulting from DAS noise, standard DAS uncertainties must be multiplied by the absolute value of Eq. (5)'s (incoming) or (6)'s (outgoing) partial derivative with respect to the raw voltage measurement:

$$\frac{\partial L_{Y\,i}}{\partial \mathrm{U}_{Y_i}} = \alpha_1 + 4c\alpha_2\sigma_{SB}\left(T_i + c\mathrm{U}_{Y_i}\right)^3 \tag{16}$$

$$u_{FDAS_{\mathrm{U}g_i}}(L_{Y_i}) = \left|\frac{\partial L_{Y\,i}}{\partial \mathrm{U}_{Y\,i}}\right| u_{FDAS}(\mathrm{U}_{Y\,i}) \tag{17}$$

The previous can be completed for individual *shortwave* radiation measurements by multiplying DAS uncertainties by the absolute value of Eq. (7)'s (incoming) or (8)'s (outgoing) partial derivative with respect to the raw voltage measurement:

$$\frac{\partial S_{Y_i}}{\partial \mathrm{P}_{Y\,i}} = \beta \tag{18}$$

$$u_{FDAS_{\mathrm{P}g_i}}(S_{Y_i}) = \left|\frac{\partial S_{Y_i}}{\partial \mathrm{P}_{Y\,i}}\right| u_{FDAS}(\mathrm{P}_{Y_i}) \tag{19}$$

Similarly, this can be calculated for the individual body temperature measurements. In the event that $R_{T_i} < 100\ [\Omega]$, the partial derivative of Eq. (2) with respect to the raw resistance measurement is computed:

CASE 1:

$$\frac{\partial T_i}{\partial R_{T_i}} = \frac{D_1(R_0-1)^3 + R_{T\,i}\left(2D_2(R_0-1)^2 + R_{T_i}\left(3D_3(R_0-1) + 4D_4R_{T_i}\right)\right)}{(R_0-1)^4} \tag{20}$$

If $R_{T_i} \geq 100\ [\Omega]$, the partial derivative of Eq. (3) with respect to the raw resistance measurement is computed:

CASE 2:

$$\frac{\partial T_i}{\partial R_{T_i}} = \frac{1}{R_0\left(A^2 - 4B(1-\frac{R_{T_i}}{R_0})\right)^{\frac{1}{2}}} \tag{21}$$

And the absolute value of the appropriate resulting value is then multiplied by the uncertainty due to DAS noise:

$$u_{FDAS_{R_{T_i}}}(T_i) = \left|\frac{\partial T_i}{\partial R_{T_i}}\right| u_{FDAS}(\mathrm{R}_{T_i}) \quad (22)$$

6.1.1.3 Body Temperature

To account for the long wave radiation emitted by the pyrgeometer, the body temperature of the pyrgeometer is calculated (Hukseflux 2007). Since the NR01's PRT is internal, it will not be directly calibrated by CVAL (as noted in Section 6.1.1), however, the combined, calibration uncertainty of the incoming and outgoing long wave radiation comprises this uncertainty. Because of this, the only quantifiable uncertainty relating to the body temperature that propagates is that introduced by the DAS.

6.1.1.4 Heater

It is assumed that any heater-induced temperature changes in the sensor will be in equilibrium with the PRT. Therefore, any measurement uncertainty induced by the heater should in theory be accounted for by the body temperature of the sensor.

6.1.1.5 Longwave radiation

The combined uncertainty for individual longwave radiation measurements can be computed with the aid of the following equations:

$$\frac{\partial L_{Y_i}}{\partial T_i} = 4\alpha_2 \sigma_{SB} (T_i + cU_i)^3 \quad (23)$$

And,

$$u_{FDAS_{R_{T_i}}}(L_{Y_i}) = \left|\frac{\partial L_{Y_i}}{\partial T_i}\right| u_{FDAS_{R_{T_i}}}(T_i) \quad (24)$$

6.1.1.6 Combined Measurement Uncertainty

The combined, standard, measurement uncertainty for a radiation measurement, given in units of W m^{-2}, is computed by summing the individual uncertainties in quadrature.

Shortwave:

$$u_c(S_{Y_i}) = \left(u^2_{CVAL}(S_{y_i}) + u^2_{FDAS}(S_{Y_i})\right)^{\frac{1}{2}} \quad (25)$$

Longwave:

$$u_c(L_{Y_i}) = \left(u_{A1,Ug}^2 + u_{FDAS}^2(L_{Y_i}) + +u_{FDAS_{R_{T_i}}}^2(L_{Y_i})\right)^{\frac{1}{2}} \quad (26)$$

$u_{A1,Ug}$ = relative uncertainty of respective (incoming / outgoing, subscript 'g') longwave radiation stream; provided by CVAL (AD[10])

Eq. (25) and (26) are direct applications of Eq. (4).

6.1.1.7 Expanded Measurement Uncertainty

The expanded uncertainties are calculated as:

$$U_{95}(X_{Y_i}) = k_{95} * u_c(X_{Y_i}) \quad (27)$$

Where,

$U_{95}(X_{Y_i})$ = respective expanded measurement uncertainty at 95% confidence ($W\ m^{-2}$)

k_{95} = 2; coverage factor for 95% confidence (unitless)

6.1.2 Uncertainty of L1 Mean Data Product

The following subsections discuss uncertainties associated with temporally averaged, i.e., L1 mean, data products. As stated previously, it is important to note the differences between the *measurement uncertainties* presented in Section 6.1.1 and the uncertainties presented in the following subsections. The uncertainties presented in the following subsections reflect the uncertainty of a time-averaged mean value, that is, they reflect the uncertainty of a distribution of measurements collected under non-controlled conditions (i.e., those found in the field), as well as any uncertainties, in the form of *Truth* and *Trueness*, related to the accuracy of the field assembly.

6.1.2.1 Repeatability (natural variation)

To quantify the uncertainty attributable to random effects, the distribution of the individual measurements is used. Specifically, the *estimated standard error of the mean (natural variation)* is computed. This value reflects the repeatability of radiation measurements for a specified time period:

$$u_{NAT}(\overline{X_Y}) = \frac{s(X_Y)}{\sqrt{n}} \quad (28)$$

Where,

$u_{NAT}(\overline{X_Y})$ = natural variation of the respective radiation data product (W m^{-2})

$s(T_B)$ = experimental standard deviation of individual observations for the defined time period (W m^{-2})

n = number of observations made during the averaging period (unitless)

6.1.2.2 Calibration

The calibration uncertainties for the respective L1 mean DPs are similar to those described in Section 6.1.1.1. However, these uncertainties, $u_{A3,Pu}$, $u_{A3,Pd}$, $u_{A3,Uw}$, and $u_{A3,Ud}$ do not account for i) individual sensor repeatability, or ii) the variation of sensors' responses over a population (reproducibility). These components of uncertainty (individually) estimate the uncertainty due to the accuracy of the instrumentation in the form of *Truth* and *Trueness*, a quantity which is not captured by the standard error of the mean. Each are provided by CVAL (AD[10]) and stored in the CI data store. The uncertainty will be applied to the *maximum* radiation value observed over the averaging period. The shortwave radiation uncertainties must be converted to measurement units first.

$$u_{CVAL(TT)}(\overline{S_Y}) = u_{A3,Pg} * P_{g_{MAX}} \quad (29)$$

Where, the subscript "MAX" represents the maximum radiation value observed over a set (averaging period) of observations. Mathematically, this can be defined as:

$$MAX = \{i: u_c(X_{Y_i}) = \max[u_c(X_{Y_1}), \ldots, u_c(X_{Y_n})]\}. \quad (30)$$

And,

$u_{CVAL(TT)}(\overline{S_Y})$ = combined, standard, Field DAS truth and trueness uncertainty due to the respective shortwave radiation measurement (W m^{-2})

$X_{Y_{MAX}}$ = respective shortwave radiation measurement corresponding to the maximum, combined, standard measurement uncertainty during the averaging period (µmol m^{-2} s^{-1})

$u_{A3,Pg}$ = Combined, relative uncertainty (truth and trueness only) of the respective radiation stream (unitless)

Note: Uncertainty values of longwave radiation do not need to be converted, as they are provided in W m^{-2}.

Please refer to AD[11] for further justification regarding evaluation and quantification of this combined uncertainty.

6.1.2.3 Field DAS

Since the L1 mean DP is a function of the individual measurements, any measurement bias introduced by the Field DAS will be reflected in the L1 mean data product. Here, the raw measurement that maximizes the combined uncertainty of an individual measurement (Eq. (30)) is used in the calculation of the L1 mean DP uncertainty. Uncertainty components due to random effects, whether a function of the environment or the measurement assembly, are quantified via the natural variation of the mean (see Section 6.1.2.1). For more information regarding the justification of this approach, please see AD[12].

The accuracy of the Field DAS in the form of *Truth* and *Trueness* propagates through to the uncertainty of the mean DP similarly to how the Field DAS uncertainty associated with a raw voltage propagates through to the uncertainty of the measurement attributable to the Field DAS.

$$u_{FDAS(TT)}\left(W_{g_{MAX}}\right) = \left(u_{V3} * W_{g_{MAX}}\right) + O_V \tag{31}$$

And

$$u_{FDAS(TT)}\left(\mathrm{R}_{T_{MAX}}\right) = \left(u_{R3} * \mathrm{R}_{T_{MAX}}\right) + O_R \tag{32}$$

Where:

$u_{FDAS(TT)}\left(W_{g_{MAX}}\right)$	= Field DAS *Truth* and *Trueness* uncertainty of $W_{g_{MAX}}$ (V)
$u_{FDAS(TT)}\left(\mathrm{R}_{T_{MAX}}\right)$	= Field DAS *Truth* and *Trueness* uncertainty of $\mathrm{R}_{T_{MAX}}$ (Ω)
$W_{g_{MAX}}$	= individual, *maximum,* radiation measurement observed during the averaging period (V)
$\mathrm{R}_{T_{MAX}}$	= individual, *maximum,* body temperature measurement observed during the averaging period (Ω)
u_{V3}	= combined, relative, Field DAS uncertainty for a voltage data stream (truth and trueness only) provided by CVAL (unitless)
u_{R3}	= combined, relative, Field DAS uncertainty for a resistance data stream (truth and trueness only) provided by CVAL (unitless)
O_V	= offset imposed by the FDAS for voltage readings provided by CVAL (V)

Thus, analogous to Eq. (17), (19), and (22), respectively:

$$u_{FDAS(TT)\,U_Y}(\overline{L_Y}) = \left|\frac{\partial L_{Y_i}}{\partial U_{Y_i}}\right|_{U_{Y_{MAX}}} u_{FDAS(TT)}(U_{Y_{MAX}}) \quad (33)$$

$$u_{FDAS(TT)}(\overline{S_Y}) = \left|\frac{\partial S_{Y_i}}{\partial P_{Y_i}}\right|_{P_{Y_{MAX}}} u_{FDAS(TT)}(P_{Y_{MAX}}) \quad (34)$$

$$u_{FDAS(TT)}(T_i) = \left|\frac{\partial T_i}{\partial R_{T_i}}\right|_{\mathrm{R}_{T_{MAX}}} u_{FDAS(TT)}(\mathrm{R}_{T_{MAX}}) \quad (35)$$

Lastly, following Eq. (24):

$$u_{FDAS(TT)\,R_T}(\overline{L_Y}) = \left|\frac{\partial L_{Y_i}}{\partial T_i}\right| u_{FDAS(TT)}(T_i) \quad (36)$$

Where,

$\left|\frac{\partial L_{Y_i}}{\partial U_{Y_i}}\right|_{U_{Y_{MAX}}}$ = partial derivative of Eq. (5) or (6) with respect to U_{Y_i} evaluated at $U_{Y_{MAX}}$ (W m^{-2})

$\left|\frac{\partial S_{Y_i}}{\partial P_{Y_i}}\right|_{P_{Y_{MAX}}}$ = partial derivative of Eq. (7) or (8) with respect to P_{Y_i} evaluated at $P_{Y_{MAX}}$ (W m^{-2})

$\left|\frac{\partial T_i}{\partial R_{T_i}}\right|_{\mathrm{R}_{T_{MAX}}}$ = partial derivative of Eq. (2) or (3) with respect to R_{T_i} evaluated at $\mathrm{R}_{T_{MAX}}$ (K)

6.1.2.4 Combined Uncertainty

The combined uncertainty for the respective L1 mean radiation data product is given in units of W m^{-2} and computed by summing the uncertainties from Sections 6.1.2.1 through 6.1.2.3 in quadrature.

Shortwave:

$$u_c(\overline{S_y}) = \left(u_{NAT}^2(\overline{S_y}) + u_{CVAL(TT)}^2(\overline{S_Y}) + u_{FDAS(TT)_{U_Y}}^2(\overline{S_Y})\right)^{\frac{1}{2}} \quad (37)$$

Longwave:

$$u_c(\overline{L_y}) = \left(u^2_{NAT}(\overline{L_y}) + u^2_{A3,Ug} + u^2_{FDAS(TT)_{U_Y}}(\overline{L_Y}) + u^2_{FDAS(TT)_{R_T}}(\overline{L_Y})\right)^{\frac{1}{2}} \quad (38)$$

6.1.2.5 Expanded Uncertainty

The expanded uncertainties are calculated as:

$$U_{95}(\overline{X_Y}) = k_{95} * u_c(\overline{X_Y}) \quad (39)$$

Where:

$U_{95}(\overline{X_Y})$ = expanded L1 mean data product uncertainty at 95% confidence (W m^{-2})

k_{95} = 2; coverage factor for 95% confidence (unitless)

6.1.2.6 Communicated Precision

L1 average shortwave radiation data products will be reported to 0.01 W m^{-2}. The FDAS is capable of measuring voltage at a resolution of 0.5 µV. Assuming a 25 µV (W m^{-2})$^{-1}$ maximum calibration sensitivity of the pyranometer, the resultant resolution of an individual shortwave measurement is 0.02 W m^{-2}. Lab-measured repeatability of the NR01 pyranometer is on the order of 0.009%.

L1 average longwave radiation data products will be reported to 0.1 W m^{-2}. Lab-measured repeatability of the NR01 pyrgeometer is on the order of 0.8 W m^{-2}.

6.2 Uncertainty Budget

The uncertainty budget is a visual aid detailing i) quantifiable sources of uncertainty, ii) means by which they are derived, and iii) the order of their propagation. Uncertainties denoted in this budget are either derived within this document or will be provided by other NEON teams (e.g., CVAL) and stored in the CI data store.

Table 5. Uncertainty budget for individual radiation measurements. Shaded rows denote the order of uncertainty propagation (from lightest to darkest).

Source of measurement uncertainty	**measurement uncertainty component $u(x_i)$**	**measurement uncertainty value (W m^{-2})**	$\frac{\partial f}{\partial x_i}$	$u_{x_i}(Y) \equiv \left\|\frac{\partial f}{\partial x_i}\right\| u(x_i)$ **(W m^{-2})**
SW radiation	$u_c(S_{Y_i})$	Eq. (25)	n/a	n/a

Sensor/calibration	$u_{CVAL}\left(S_{y_i}\right)$	Eq. (13)	1	Eq. (13)
FDAS (voltage)	$u_{FDAS}\left(P_{g_i}\right)$	Eq. (14) (V)	Eq. (18)	Eq. (19)
LW radiation	$u_c\left(L_{Y_i}\right)$	Eq. (26)	n/a	n/a
Sensor/calibration	$u_{A1,Ug}$	AD[10]	1	AD[10]
FDAS (voltage)	$u_{FDAS}\left(U_{g_i}\right)$	Eq. (22) (V)	Eq. (23)	Eq. (24)
Body temperature	$u_{FDAS_{R_{T_i}}}\left(T_i\right)$	Eq. (22) (K)	Eq. (23)	Eq. (24)
FDAS (resistance)	$u_{FDAS}\left(\mathrm{R}_{T_i}\right)$	Eq. (15) (Ω)	Eq. (20) OR (21)	Eq. (22) (K)

Table 6. Uncertainty budget for L1 mean radiation DPs. Shaded rows denote the order of uncertainty propagation (from lightest to darkest).

Source of uncertainty	**uncertainty component $u(x_i)$**	**uncertainty value (W m^{-2})**	$\frac{\partial f}{\partial x_i}$	$u_{u_{x_i}}(Y) \equiv \left\|\frac{\partial f}{\partial x_i}\right\| u(x_i)$ **(W m^{-2})**
SW radiation	$u_c\left(\overline{S_Y}\right)$	Eq. (37)	n/a	n/a
Natural variation	$u_{NAT}\left(\overline{S_Y}\right)$	Eq. (28)	1	Eq. (28)
Sensor/calibration	$u_{CVAL(TT)}\left(\overline{S_Y}\right)$	Eq. (29)	1	Eq. (29)
FDAS (Voltage)	$u_{FDAS(TT)}\left(P_g\right)$	Eq. (31) (V)	Eq. (18)	Eq. (34)
LW radiation	$u_c\left(\overline{L_Y}\right)$	Eq. (38)	n/a	n/a
Natural variation	$u_{NAT}\left(\overline{L_Y}\right)$	Eq. (28)	1	Eq. (28)
Sensor/calibration	$u_{A3,Ug}$	AD[10]	1	AD[10]
FDAS (Voltage)	$u_{FDAS(TT)}\left(U_g\right)$	Eq. (31) (V)	Eq. (16)	Eq. (33)
Sensor body	$u_{FDAS(TT)}\left(T_i\right)$	Eq. (35) (K)	Eq. (23)	Eq. (36)
FDAS (resistance)	$u_{FDAS(TT)}\left(T_i\right)$	Eq. (32) (Ω)	Eq. (20) OR (21)	Eq. (35) (K)

7 FUTURE PLANS AND MODIFICATIONS

Details concerning the evaluation and quantification of Sensor and Field DAS drift will be added to the uncertainty section.

QA/QC tests may be expanded to include consistency analyses among similar measurement streams.

8 BIBLIOGRAPHY

ASTM E1137 (2004) Standard Specification for Industrial Platinum Resistance Thermometers. pp. 7. ASTM International, West Conshohocken, PA, USA. DOI: 10.1520/E1137_E1137M-04

Campbell Scientific (2008) NR01 four-component net radiation sensor instruction manual. pp. 40. Campbell Scientific, Logan, Utah, USA.

Fu, Q. (2003). Encyclopedia of atmospheric sciences: radiation (solar) (eds *J. R. Holton, J. Pyle, & J. A. Curry)*, pp. 1859-1863. Academic Press, London. ISBN-10: 0122270908

Goody, R.M. & Yung, Y. L. (1995) Atmospheric radiation: theoretical basis. 2nd Ed. pp. 544. Oxford University Press, Oxford, UK ISBN-10: 0195102916

Hukseflux (2007) NR01 RA01 manual version 0715. pp. 40. Hukseflux Thermal Sensors, Netherlands

Joint Committee for Guides in Metrology (JCGM) (2008) Evaluation of measurement data – Guide to the expression of uncertainty in measurement. pp. 120.

Joint Committee for Guides in Metrology (JCGM) (2012) International vocabulary of metrology – Basic and general concepts and associated terms (VIM). 3rd Ed. pp. 92

National Renewable Energy Laboratory (NREL) (2013) Pyrgeometer Calibration for DOE – Atmospheric System Research Program Using NREL Method. [Available online at : http://www.nrel.gov/docs/fy10osti/47756.pdf]

Taylor, J. R. (1997) An Introduction to Error Analysis: The Study of Uncertainties in Physical Measurements. 2nd Ed. pp. 327. University Science Books, Mill Valley, California, USA.